Acta Pharmacologica Sinica (2016) 37: 1281–1297
 1671-4083/16
www.nature.com/aps

Original Article

Small molecule LX2343 ameliorates cognitive deficits in AD model mice by targeting both amyloid β production and clearance

Xiao-dan GUO[1, 2, 3], Guang-long SUN[1, 2, 3], Ting-ting ZHOU[1, 2, 3], Xin XU[1, 2, 3], Zhi-yuan ZHU[1, 2, 3], Vatcharin RUKACHAISIRIKUL[4], Li-hong HU[1, 2, 3, *], Xu SHEN[1, 2, 3, *]

[1]CAS Key Laboratory of Receptor Research and [2]State Key Laboratory of Drug Research, Shanghai Institute of Materia Medica, Chinese Academy of Sciences, Shanghai 201203, China; [3]University of Chinese Academy of Sciences, Beijing 100049, China; [4]Department of Chemistry, Faculty of Science, Prince of Songkla University, Hat Yai, Songkhla 90112, Thailand

Aim: Streptozotocin (STZ) is widely used to induce oxidative damage and to impair glucose metabolism, apoptosis, and tau/Aβ pathology, eventually leading to cognitive deficits in both *in vitro* and *in vivo* models of Alzheimer's disease (AD). In this study, we constructed a cell-based platform using STZ to induce stress conditions mimicking the complicated pathologies of AD *in vitro*, and evaluated the anti-amyloid effects of a small molecule, N-(1,3-benzodioxol-5-yl)-2-[5-chloro-2-methoxy(phenylsulfonyl)anilino]acetamide (LX2343) in the amelioration of cognitive deficits in AD model mice.
Methods: Cell-based assays for screening anti-amyloid compounds were established by assessing Aβ accumulation in HEK293-APP_{sw} and CHO-APP cells, and Aβ clearance in primary astrocytes and SH-SY5Y cells after the cells were treated with STZ in the presence of the test compounds. Autophagic flux was observed using confocal laser scanning microscopy. APP/PS1 transgenic mice were administered LX2343 (10 $mg{\cdot}kg^{-1}{\cdot}d^{-1}$, ip) for 100 d. After LX2343 administration, cognitive ability of the mice was evaluated using Morris water maze test, and senile plaques in the brains were detected using Thioflavine S staining. ELISA assay was used to evaluate Aβ and sAPPβ levels, while Western blot analysis was used to measure the signaling proteins in both cell and animal brains.
Results: LX2343 (5–20 μmol/L) dose-dependently decreased Aβ accumulation in HEK293-APP_{sw} and CHO-APP cells, and promoted Aβ clearance in SH-SY5Y cells and primary astrocytes. The anti-amyloid effects of LX2343 were attributed to suppressing JNK-mediated APP^{Thr668} phosphorylation, thus inhibiting APP cleavage on one hand, and inhibiting BACE1 enzymatic activity with an IC_{50} value of 11.43±0.36 μmol/L, on the other hand. Furthermore, LX2343 acted as a non-ATP competitive PI3K inhibitor to negatively regulate AKT/mTOR signaling, thus promoting autophagy, and increasing Aβ clearance. Administration of LX2343 in APP/PS1 transgenic mice significantly ameliorated cognitive deficits and markedly ameliorated the Aβ pathology in their brains.
Conclusion: LX2343 ameliorates cognitive dysfunction in APP/PS1 transgenic mice via both Aβ production inhibition and clearance promotion, which highlights the potential of LX2343 in the treatment of AD.

Keywords: Alzheimer's disease; N-(1,3-benzodioxol-5-yl)-2-[5-chloro-2-methoxy(phenylsulfonyl)anilino]acetamide (LX2343); streptozotocin; amyloid β; BACE1; PI3K; autophagy; APP/PS1 transgenic mice; cognitive deficit

Acta Pharmacologica Sinica (2016) 37: 1281–1297; doi: 10.1038/aps.2016.80; published online 29 Aug 2016

Introduction

Alzheimer's disease (AD) is characterized as a progressively neurodegenerative disorder and results in an irreversible loss of neurons and further intellectual abilities including memory and reasoning[1]. By accounting for approximately 70%, AD has become the most common form of dementia of the aged population, and the worldwide epidemic of this disease has severely threatened the elderly and brought economic burdens to society[2]. Currently, several hypotheses have been proposed to elucidate AD pathogenesis, and the Aβ hypothesis is accepted as one of the most likely evidence-based mechanisms, as supported by the discovery of senile plaques in postmortem brains[3]. According to Aβ hypothesis, the Aβ generated from the sequential proteolytic cleavage of amyloid precursor protein (APP) by β- and γ-secretases, is the root cause of AD, and accumulation of Aβ outside the neurons in the brain leads to a series of harmful events involving the for-

*To whom correspondence should be addressed.
E-mail xshen@mail.shcnc.ac.cn (Xu SHEN);
lhhu@simm.ac.cn (Li-hong HU)
Received 2016-03-02 Accepted 2016-05-30

mation of plaques and neurofibrillary tangles of hyperphosphorylated tau, neuronal apoptosis, concomitant inflammation and oxidative stress[4]. Therefore, targeting Aβ is considered a promising strategy for anti-AD drug discovery[5].

Aβ in the brain exists in a dynamic equilibrium of Aβ production and clearance, and imbalance of this equilibrium may cause dysfunction of Aβ metabolism resulting in Aβ aggregation[4, 6]. It has been suggested that the agents able to suppress Aβ production/aggregation or enhance Aβ clearance may show promise for AD therapy[5, 7], and α-, β-, and γ-secretases, the three important enzymes mediating the production of Aβ, are generally considered the key targets for drug discovery against AD[8–10]. To date, many compounds targeting secretases have been developed, some of which have even entered clinical trials[9, 11, 12]. However, despite the great efforts devoted to the drug discovery based on Aβ hypothesis, the growing number of failed clinical trials has caused people to argue against this assumption of Aβ[13].

AD is a disease linked to age, and over 90% of AD cases are first diagnosed after age 65. Disease onset at earlier ages is rare and usually associated with genetic mutations[14]. It has been identified that mutations of the genes APP, PSEN1 and PSEN2 are tightly involved in familial AD, while sporadic AD, which is more prevalent, does not always target APP or secretase genes as risk factors[15]. In fact, AD is characterized by complicated pathogenesis involving multiple aberrant signaling genes and pathways[16]. Research has demonstrated that oxidative imbalance is one of the manifestations of AD even preceding Aβ deposition and plays a crucial role in neuronal degeneration[17]. Persistent oxidative stress aggravates the production and aggregation of Aβ and promotes tau phosphorylation[18, 19]. In addition, hyperphosphorylated tau, another key hallmark of AD pathology, has also been determined to cause oxidative stress and mediate Aβ toxicity[20]. Moreover, Aβ exacerbates oxidative stress by increasing reactive oxygen species (ROS) and damaging mitochondrial morphology and function and triggers tau aggregation and downstream toxicity[4]. Thus, the interplay among these pathogenic events induces a vicious cycle between oxidative stress and Aβ deposition, thereby accelerating the progression of AD.

The above mentioned facts suggest the potency of the discovery of anti-amyloid agents under a platform involving multiple pathological events. Considering that streptozotocin (STZ) has been widely used to induce oxidative damage and to impair glucose metabolism, apoptosis, and tau/Aβ pathology, eventually leading to cognitive deficits in both *in vitro* and *in vivo* models[21–23], we constructed a cell-based platform in the present study for anti-amyloid compound screening using STZ to induce stress conditions mimicking the complicated pathologies of AD *in vitro*. Finally, by screening lab in-house small compound library, we discovered N-(1,3-benzodioxol-5-yl)-2-[5-chloro-2-methoxy(phenylsulfonyl)anilino]acetamide (LX2343, Figure 1A). LX2343 alleviated Aβ levels by both activating its clearance and inhibiting its production under STZ-induced pathological conditions. The mechanisms underlying the LX2343-mediated effects were intensively investigated. Moreover, assays in APP/PS1 transgenic AD model mice verified the amelioration of AD-relevant pathogenesis and cognitive deficits by LX2343. Our results thus highlight the potential of LX2343 in the treatment of AD.

Materials and methods

Materials

All cell culture reagents were purchased from Gibco (Invitrogen, USA). STZ, wortmannin and chloroquine were purchased from Sigma-Aldrich (USA). Idelalisib (CAL101) was purchased from Selleck (USA), and LX2343 was obtained from the commercial SPECS compound library (SPECS, Netherlands).

Cell culture

SH-SY5Y cells were grown in a mixture 1:1 of Dulbecco's modified Eagle's medium and Ham's F-12 (DMEM/F12) supplemented with 10% fetal bovine serum (FBS) and 100 unit/mL penicillin-streptomycin. HEK293 cells expressing APP Swedish mutant$^{K595N/M596L}$ (HEK293-APP$_{sw}$) (kindly provided by Prof Gang PEI, Shanghai Institutes for Biological Sciences, China) were grown in DMEM containing 10% FBS and 100 unit/mL penicillin-streptomycin. CHO cells expressing APP and BACE1 (CHO-APP) were grown in Ham's F12 containing 10% FBS and 100 unit/mL penicillin-streptomycin. All cells were cultured in a humidified incubator with 5% CO_2 at 37 °C.

Primary cortical astrocyte culture

Primary cortical astrocytes were prepared according to the published approach[24]. Briefly, cerebral cortices were separated from the brain, minced into small pieces, digested with D-Hanks buffer (5.4 mmol/L KCl, 0.41 mmol/L KH_2PO_4, 138 mmol/L NaCl, 4.5 mmol/L $NaHCO_3$, 0.22 mmol/L Na_2HPO_4, pH7.4) containing 0.125% trypsin and 200 U/mL Dnase (Sigma-Aldrich, USA), and incubated for 15 min at 37 °C. Then, the dissociated cells were cultured in DMEM/F12 with 10% FBS and 50 U/mL PS using a poly-D-lysine-coated 75 cm^2 flask at a density of 200 000 cells/cm^2. After 7 d, the flask was rotated at 220 rounds per minute overnight at 37 °C, and the remaining adhered cells were selected by Ara-C (cytosine β-D-arabinofuranoside, Sigma-Aldrich, USA) treatment and were identified as astrocytes using GFAP and DAPI staining.

STZ preparation

Considering that STZ is a hydrophilic compound that is soluble in water and stable at an acidic pH of 4.5 but becomes damaged and degrades at higher pH[25], STZ was thus reconstituted in 0.1 mol/L ice-cold citrate buffer (pH 4.5) and aliquoted to avoid repeated freeze/thaw cycles. The stocks were stored in the dark at -20 °C up to 30 d to ensure its stability.

Confocal laser scanning microscopy (CLSM) assay

Stimulation by LX2343 on autophagy was evaluated using a mRFP-GFP-LC3 translocation assay. Briefly, SH-SY5Y cells were transfected with mRFP-GFP-LC3 plasmids via an adenovirus (Hanbio, China). The cells were treated without or

with STZ (0.8 mmol/L) in combination with 5 or 20 μmol/L LX2343 for 4 h and then fixed with 4% paraformaldehyde and observed using an Olympus Fluoview FV1000 confocal microscope (Olympus, Japan).

BACE1 enzymatic activity assay

Inhibition of BACE1 enzyme by LX2343 was assayed using BACE1 activity kits (Invitrogen, USA) *in vitro* according to the manufacturer's protocol. Briefly, BACE1 substrate (250 nmol/L), BACE1 enzyme (0.35 U/mL), and varied concentrations of LX2343 (5, 10, and 20 μmol/L) were sequentially incubated for 1 h at 37 °C in the dark. Fluorescence intensity was measured with excitation and emission wavelengths at 545 and 585 nm, respectively.

PI_3-kinase enzymatic activity assay

Inhibition PI_3-kinase (PI_3K) enzyme by LX2343 was assayed using PI_3-kinase activity ELISA kits (Echelon, USA) according to the manufacturer's protocol.

Western blot

In cell-based assays, SH-SY5Y cells, HEK293-APP_{sw} cells, CHO-APP cells or primary astrocytes were exposed to STZ (0.8 mmol/L for SH-SY5Y cells and 0.4 mmol/L for the other cells), treated with different concentrations of LX2343 (5, 10, and 20 μmol/L), and then lysed with RIPA buffer (Thermo, USA) containing a protease inhibitor cocktail (Thermo, USA). Protein concentrations were determined using BCA protein assay kits (Thermo, USA). Proteins were mixed with 2× SDS-PAGE sample buffer (25% SDS, 62.5 mmol/L Tris-HCl, pH 6.8, 25% glycerol, 0.5 mol/L DTT and 0.1% Bromophenol Blue) and then boiled for 15 min at 99 °C.

In brain tissue-based assays, the brain tissues of four mice from each group were homogenized with RIPA buffer (Thermo, USA) containing a protease inhibitor cocktail and phosphatase inhibitor cocktails (Thermo, USA) using a hand-hold motor and kept on ice for 1 h to completely lyse the cells. The homogenates were then centrifuged at 20 000×*g* and 4 °C for 30 min. The supernatants were collected, and protein concentration was determined using BCA protein assay kits. Equal amounts of lysates (4 mg/mL protein) were mixed with 2× SDS-PAGE sample buffers and then boiled for 15 min at 99 °C.

Antibodies against P-JNK, JNK, P-PI_3K, PI_3K, P-AKT, AKT, P-mTOR, mTOR, P-ULK1, ULK1, P-P70S6K, P70S6K, p62, P^{668}-APP, PSD95, synaptophysin, VAMP2 and GAPDH were obtained from Cell Signaling Technology (USA). Antibodies against BACE1 and ADAM10 were purchased from Sigma-Aldrich (USA). An antibody against sAPPβ was purchased from Convance (USA). For Western blot assays, cells or tissue extracts were separated using SDS-PAGE and transferred to polyvinylidene difluoride membrane filters (GE, USA). After incubation with the corresponding antibodies overnight, the blots were visualized using a Dura detection system (Thermo, USA).

Intracellular Aβ clearance assay

Intracellular Aβ clearance in SH-AY5Y cells or astrocytes was detected according to the Landreth approach[26, 27]. Briefly, SH-SY5Y cells or astrocytes were sequentially cultured with varied concentrations of LX2343 (5, 10, and 20 μmol/L) and STZ (0.8 mmol/L for SH-SY5Y cells, 0.4 mmol/L for astrocytes) for 4 h and then cells were treated with 2 μg/mL soluble $A\beta_{40}$ for 3 h, followed by lysis in 50 mmol/L Tris buffer containing 1% SDS and a protease inhibitor cocktail. Protein concentration was determined using BCA protein assay kits, and intracellular Aβ peptide was evaluated using ELISA and normalized to the total protein.

ELISA assay

In cell-based assays, HEK293-APP_{sw} or CHO-APP cells were incubated with different concentrations of LX2343 (5, 10, and 20 μmol/L) and STZ (0.4 mmol/L) for 8 h. The cell culture media were collected, and a complete protease inhibitor cocktail was added (Thermo, USA). The culture media were then centrifuged at 20 000×*g* and 4 °C for 10 min, and the supernatants were collected. ELISA kits of $A\beta_{40}$/$A\beta_{42}$ (Invitrogen, USA) and sAPPβ (Immunobiological Laboratories, Japan) were used to evaluate $A\beta_{40}$, $A\beta_{42}$, and sAPPβ levels, respectively.

For brain assays, hippocampal or cortical samples were prepared according to the published approach[28]. In brief, each sample was homogenized in a mixture containing 5 mol/L guanidine hydrogenchloride and a complete protease inhibitor cocktail (Thermo, USA) using a hand-hold motor, and the homogenates were then centrifuged at 20 000×*g* and 4 °C for 30 min. The supernatants were collected, and the $A\beta_{40}$ and $A\beta_{42}$ levels were tested according to the protocol of the $A\beta_{40}$/$A\beta_{42}$ ELISA kits.

Animal experiment

All animal experiments were performed according to the Institutional Ethical Guidelines of Shanghai Institute of Materia Medica, Chinese Academy of Sciences, on animal care.

APP/PS1 [B6C3-Tg(APP_{swe}, $PS1^{dE9}$)] transgenic mice were purchased from Jackson Laboratory (Bar Harbor, ME, USA). Genotyping to confirm APP/PS1 DNA sequences in their offspring was performed by assaying the DNA from tail biopsies, with Tg-negative mice as a negative control[29]. The transgenic mice were housed under standard conditions including a 12 h light/dark cycle at a room temperature of 22 °C. As described previously, APP/PS1 mice exhibited early AD symptoms at 6 to 7 months of age and developed more serious symptoms after more than three months[30]. In the current study, twenty male APP/PS1 mice were divided into two groups with ten non-transgenic mice in one group to serve as a negative control. LX2343 was dissolved in 3% DMSO and 5% tween-80. The two 6-month transgenic groups were administered 10 $mg \cdot kg^{-1} \cdot d^{-1}$ of LX2343 or vehicle, and the 6-month non-transgenic group was administered the vehicle for 100 d via intraperitoneal injection. After 100 d of administration, MWM assays were applied to evaluate the cognitive abilities of the

mice for 8 d under continuous LX2343 treatment. Upon completion of the MWM test, the mice were euthanized, and the brains were removed and bisected at the mid-sagittal plane. The right hemispheres were frozen and stored at -80 °C, and the left hemispheres were fixed in 4% paraformaldehyde.

MWM test

MWM tests were carried out as previously described[28]. Briefly, for the training trials, the mice were trained to find an invisible submerged white platform in a circular pool (120 cm in diameter, 50 cm deep) filled with milk-tinted water using a variety of visual cues located on the pool walls; training was performed for 3 trials per day for 8 consecutive days. For each trial, mice were given 90 s to find the invisible platform. Each mouse was allowed to stay on the platform for 15 s if the mouse found the platform within the given time. If the mouse failed to find the platform within the given time, they were manually placed to the platform and kept there for 15 s. On the last day, after the training trials, a probe trial was performed by removing the platform, and the animals were allowed to swim for 90 s to search for it. All data were collected for the animal performance analysis. For data analysis, the pool was divided into four equal quadrants formed by imaging lines, which intersected the center of the pool at right angles, and the quadrants were termed north, south, east and west.

Thioflavine S staining assay

The paraformaldehyde-fixed brain tissues (around thirty-five mm thick) were obtained and embedded in paraffin. Five-micrometer-thick coronal sections were used for Thioflavine S staining according to a previous approach[28]. For Thioflavine S staining, the sections were de-paraffinized, hydrated and stained in a 1% Thioflavine S staining stock for 5 min, differentiated in 70% alcohol for 5 min and then mounted in glycerin jelly.

Thioflavine S plaque burdens were determined separately in the hippocampus and cortex. Thioflavine S plaque burdens were counted on every five fields throughout the entire hippocampus and cortex using Image-Pro Plus (Media Cybernetics).

Wild-type *Drosophila melanogaster* culture and lifespan experiment

yw D melanogaster was used in this study. *Drosophila melanogastes* were maintained, and all experiments were conducted at 25 °C and at 60% relative humidity on a 12 h:12 h light-dark cycle using standard SY food (10% sucrose, 10% yeast, 1.5% agar). On the second day after eclosion, male *Drosophila melanogastes* were selected and sorted into different vials (30 *Drosophila melanogastes*/vial) for drug feeding. LX2343 was dissolved in DMSO and added to SYA food at appropriate concentrations (10 or 20 μmol/L). For control food, DMSO alone was added. Initially, there were 120 *Drosophila melanogastes* in each group. *Drosophila melanogastes* were transferred to new vials every 2 d and scored for deaths.

Liver function

The serum levels of alanine aminotransferase (ALT), aspartate aminotransferase (AST), total protein (TP) and the albumin (ALB) were measured using an auto-biochemical analyzer (Hitachi, Japan).

Statistical analysis

The significant differences between the multiple treatments and control were analyzed using a one-way ANOVA followed by Dunnett's *post-hoc* tests or *t* tests. *P* values less than 0.05 were considered statistically significant.

Results

LX2343 inhibited Aβ production

LX2343 reversed the STZ-induced Aβ accumulation

In screening for the agents able to alleviate Aβ burden under pathological conditions against the lab's in-house compound library, STZ was applied as a stimulator, and ELISA assays were performed in both HEK293-APP_{sw} and CHO-APP cells. Based on random screening to target Aβ content, small molecule LX2343 was finally identified. ELISA results demonstrated that STZ increased Aβ accumulation, and LX2343 treatment effectively antagonized Aβ deposition in both HEK293-APP_{sw} (Figure 1B, 1C) and CHO-APP (Figure 1D, 1E) cells.

LX2343 reduced Aβ production involving JNK/APP^{Thr668} pathway inhibition

According to previously published reports, APP has an MAP kinase phosphorylation site at Thr668[31], which is vulnerable to c-Jun N-terminal kinase (JNK) activation that promotes amyloidogenic cleavage of APP in neurons, thereby resulting in Aβ generation[32, 33]. This finding is highlighted by the evidence of hyperphosphorylated APP^{Thr668} in human AD brains[33]. Therefore, inhibition of JNK-mediated APP^{Thr668} phosphorylation has been proposed as a strategy to prevent Aβ production[7]. Accordingly, we investigated the potential of LX2343 in the regulation of the JNK/APP^{Thr668} pathway in response to Aβ generation. Interestingly, we found that STZ treatment caused increases in JNK phosphorylation, APP^{Thr668} phosphorylation and the levels of sAPPβ, a direct product of APP by β-secretase (also known as BACE1) cleavage, in both HEK293-APP_{sw} cells (Figure 2A, 2B) and CHO-APP cells (Figure 2C, 2D), and LX2343 incubation antagonized all of these STZ-induced stimulations dose-dependently. Furthermore, ELISA assays were performed to quantitatively detect sAPPβ levels as an indication of Aβ production[31]. As expected, sAPPβ levels in both HEK293-APP_{sw} and CHO-APP cells were effectively decreased upon LX2343 treatment compared with the level in STZ-treated cells (Figure 2E, 2F). Thus, these results indicated that JNK/APP^{Thr668} pathway inhibition was involved in LX2343-reduced Aβ production.

LX2343 as a BACE1 enzymatic inhibitor suppressed Aβ production

Next, considering that BACE1 as a rate-limiting enzyme plays an important role in Aβ production[1], we also investigated

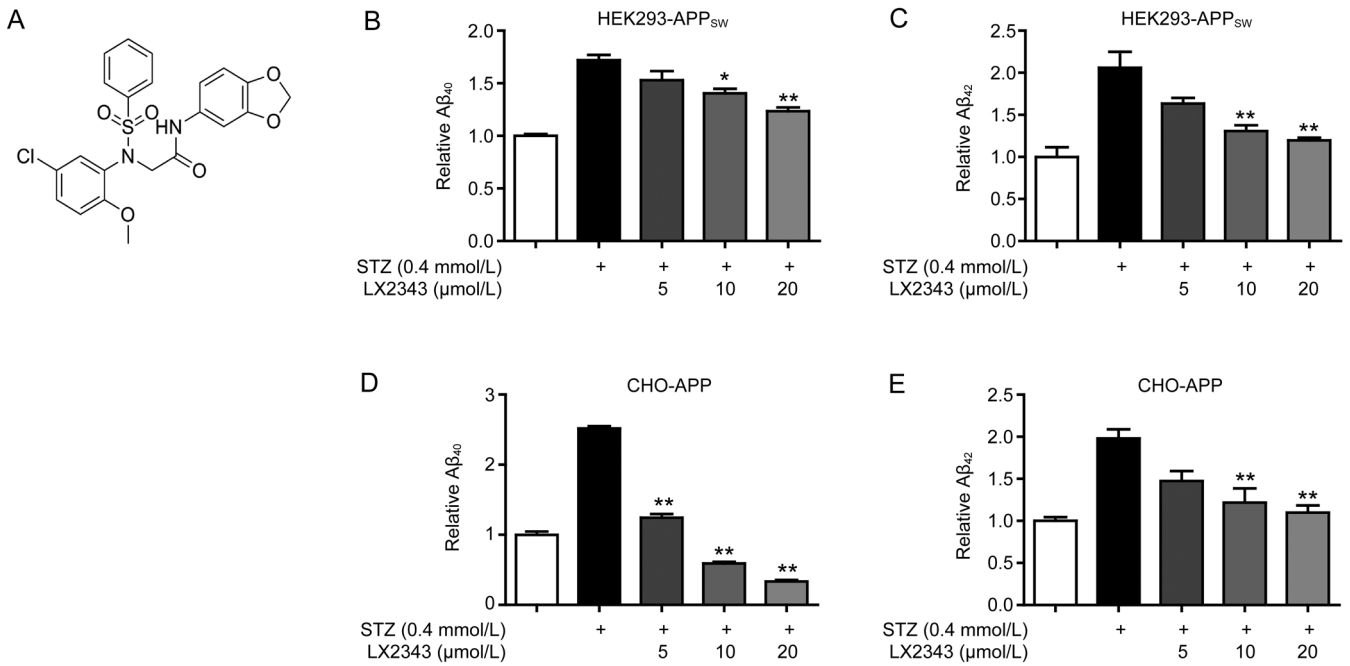

Figure 1. LX2343 effectively reversed STZ-induced Aβ accumulation. Structure of LX2343 (A). ELISA assays of LX2343-induced $A\beta_{40}$ or $A\beta_{42}$ decrease in HEK293-APP_{sw} (B, C) and CHO-APP (D, E) cells (one-way ANOVA, Dunnett's multiple comparison test. n=3. $^{*}P$<0.05, $^{**}P$<0.01 *vs* STZ). All data were obtained from three independent experiments and are presented as the mean±SEM.

whether LX2343 exhibited any effects on BACE1 relating to its expression and activity. Interestingly, Western blot results in both HEK293-APP_{sw} cells and CHO-APP cells demonstrated that LX2343 failed to regulate BACE1 protein levels (Figure 2A–2D), while *in vitro* BACE1 enzymatic activity assays indicated that LX2343 dose-dependently decreased BACE1 activity (Figure 2G, TDC as a positive control[28]) with an IC_{50} of 11.43±0.36 μmol/L (Figure 2H). Therefore, these results demonstrated that LX2343 functioned also as a BACE1 enzymatic inhibitor in suppressing Aβ production.

LX2343 had no effects on non-amyloidogenic processing of APP

Given that the proteolytic process of APP involves amyloidogenic or non-amyloidogenic pathways[11] and that α-secretase as a main protease in the non-amyloidogenic pathway also cleaves APP within the Aβ domain, leading to competition with BACE1 for the initial cleavage of APP and to the opposite effect on Aβ generation[11], the effect of LX2343 on the non-amyloidogenic process of APP through α-secretase regulation was also detected here. Our results indicated that LX2343 had no effects on the expression of ADAM10, the potent enzyme involved in α-secretase activity (Figure 3A–3D), or on the level of sAPPα, the α-cleavage product of APP (Figure 3E, 3F) in both HEK293-APP_{sw} cells and CHO-APP cells.

Taken together, both JNK/APP^{The668} pathway regulation and BACE1 enzymatic inhibition are implicated in LX2343-reduced Aβ production.

LX2343 promoted exogenous Aβ clearance

Because Aβ levels involve a dynamic equilibrium between Aβ production and clearance, we also investigated the potential effect of LX2343 on exogenous Aβ clearance in SH-SY5Y cells and in primary astrocytes. The results indicated that LX2343 dose-dependently enhanced exogenous Aβ clearance in both SH-SY5Y cells (Figure 4A, 4B) and in primary astrocytes (Figure 4C, 4D).

LX2343 stimulated autophagy in the promotion of Aβ clearance by inhibiting the PI_3K/AKT/mTOR pathway

Next, we attempted to investigate the mechanism underlying the stimulation of LX2343 in Aβ clearance. In this assay, we focused on an autophagy-relevant study because autophagy as a potent catabolic process is highly correlated with the regulation of Aβ clearance[34]. Published results have indicated that activation of the mammalian target of rapamycin (mTOR), a conserved Ser/Thr protein kinase, disrupts autophagy via phosphorylation of the Unc51-like kinase 1 (ULK1), which is an initiator of the autophagy process[35]. AKT (protein kinase B, PKB) is a positive regulator of mTOR and increases mTOR activity through direct or indirect phosphorylation of mTOR[36, 37], whereas AKT is regulated by phosphoinositide 3-kinase (PI_3-kinase, PI_3K)[38]. Therefore, the PI_3K/AKT pathway is tightly linked to mTOR-mediated autophagy regulation and further Aβ clearance.

Thus, we at first examined the regulation of LX2343 against the PI_3K/AKT-mediated autophagy pathway. In this assay, STZ was used as an autophagy inhibitor according to the published result that STZ disrupts the autophagy process in renal and cardiac tissues[39, 40] and in diabetic neuropathy models[23]. The incubation time of STZ with SH-SY5Y cells or primary

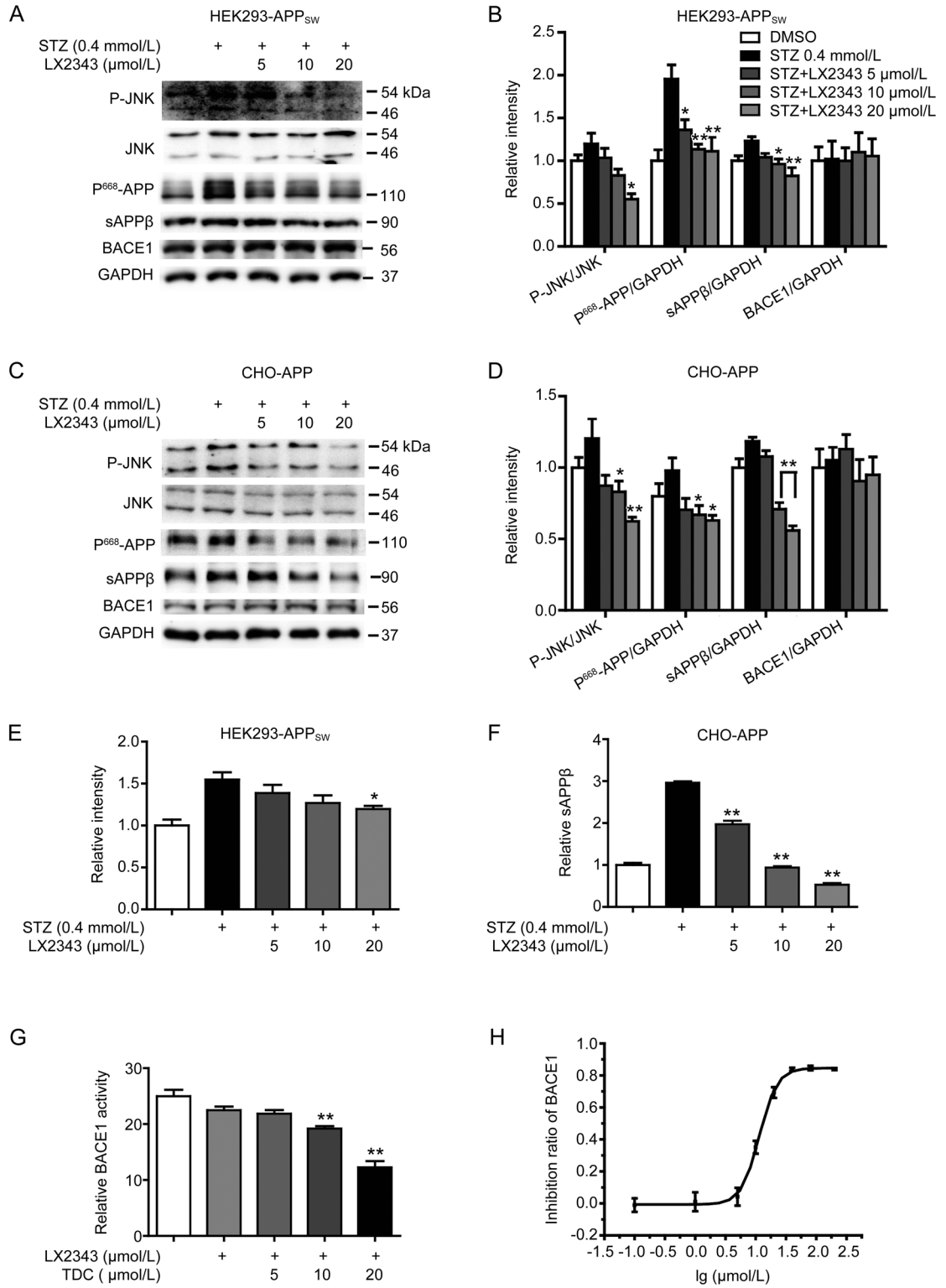

Figure 2. LX2343 reduced Aβ production involving both JNK/APP^{Thr668} pathway regulation and BACE1 enzymatic inhibition. Western blotting and its quantification results demonstrated that LX2343 reduced the phosphorylation of JNK and APP^{Thr668}, decreased the protein level of sAPPβ, and had no effects on the protein level of BACE1 in HEK293-APP$_{sw}$ (A, B) and CHO-APP (C, D) cells (one-way ANOVA, Dunnett's multiple comparison test. n=3. $^{*}P$<0.05, $^{**}P$<0.01 *vs* STZ). ELISA results indicated that LX2343 decreased sAPPβ in HEK293-APP$_{sw}$ and CHO-APP cells (E, F) (one-way ANOVA, Dunnett's multiple comparison test. n=3. $^{*}P$<0.05, $^{**}P$<0.01 versus STZ). LX2343 inhibited BACE1 activity with an IC$_{50}$ of 11.43±0.36 μmol/L *in vitro*, and LX2343 concentration is expressed on a log$_{10}$ scale (G, H) (TDC[28]: 2,2′,4′-trihydroxychalcone, BACE1 non-competitive inhibitor. One-way ANOVA, Dunnett's multiple comparison test. $^{**}P$<0.01 *vs* DMSO; TDC, *t* test. n=3). GAPDH was used as loading control in the Western blot assays. All data were obtained from three independent experiments and are presented as the mean±SEM.

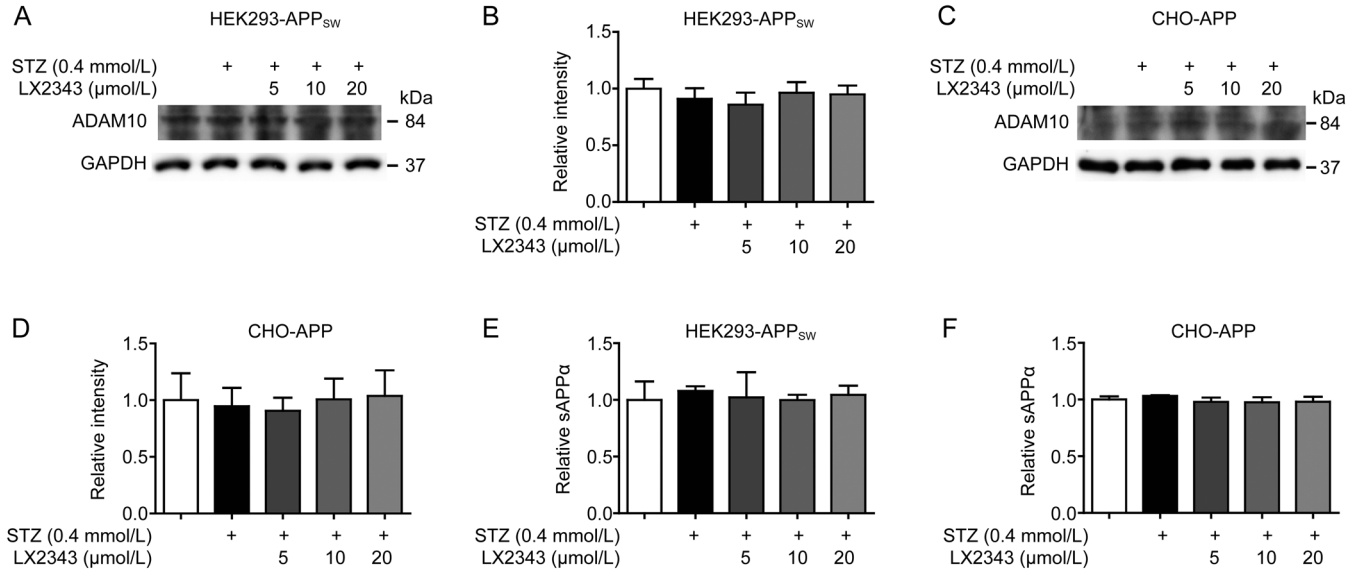

Figure 3. LX2343 had no effects on non-amyloidogenic processing of APP. Western blotting and its quantification results demonstrated that LX2343 had no effects on ADAM10 in HEK293-APP_{sw} and CHO-APP cells (A–D) (one-way ANOVA, Dunnett's multiple comparison test, n=3). Intracellular sAPPα level was evaluated using ELISA assay (E, F) (one-way ANOVA, Dunnett's multiple comparison test, n=3). GAPDH was used as loading control in Western blot assays. All data were obtained from three independent experiments and presented as means±SEM.

astrocytes was set to 4 h based on a previously published study[41] and on our result (Figure 5A, 5B) that STZ stimulation led to increased phosphorylation of AKT in a short time but presented a decrease in AKT phosphorylation upon extended periods of time. Accordingly, we also selected STZ stimulation at 4 h to perform the follow-up assays in the current study. As expected, the results of both the SH-SY5Y cells (Figure 5C–5E) and primary astrocytes (Figure 5F–5H) indicated the capability of LX2343 to stimulate PI_3K/AKT/mTOR-mediated autophagy, in that LX2343 dose-dependently reversed STZ-induced increases in the phosphorylation of PI_3K, AKT, mTOR, P62[42], ULK1, and P70S6K and antagonized the STZ-induced repression of LC3II[43] levels in both types of cells.

Moreover, to verify the stimulation of LX2343 on the autophagy process, confocal laser scanning microscopy (CLSM) assays were also employed to investigate the potential effects of LX2343 on autophagic flux and autolysosome formation in SH-SY5Y cells by using an expression vector encoding mRFP-GFP fluorescence-tagged LC3 (mRFP-GFP-LC3). In the assay, when mRFP-GFP-LC3 was localized to autophagosomes, both red (mRFP) and green (GFP) signals were emitted, which merged as yellow. Notably, when autophagosomes fused with lysosomes, forming acidic autolysosomes, the co-located mRFP-GFP-LC3 emitted only a red signal because the green signal quenched immediately under acidic conditions[43]. Compared with control cells, STZ significantly decreased the numbers of both $mRFP^+$-GFP^+ yellow and $mRFP^+$-GFP^- red puncta, and LX2343 dose-dependently increased the amount of both types of puncta (Figure 6A). These results thus confirmed that LX2343 promoted autolysosome formation and autophagic flux. Taken together, all of the results suggested that LX2343 stimulated PI_3K/AKT/mTOR pathway-mediated autophagy.

Next, we investigated whether the LX2343-induced autophagy activation was responsible for its stimulation of Aβ clearance. The autophagy inhibitor chloroquine (CQ[44]) was applied to an assay of SH-SY5Y cells. The cells were exposed to STZ, followed by treatment with LX2343, CQ, or LX2343 combined with CQ, and then co-incubated with adscititious Aβ. Intracellular Aβ peptide was thus evaluated using ELISA. As expected, CQ partly reversed the LX2343-induced Aβ reduction (Figure 6B). This result thereby demonstrated that stimulation with LX2343 induced A clearance via activation of autophagy.

LX2343 was a non-ATP competitive PI_3K inhibitor

Because LX2343 has been determined to inhibit PI_3K/AKT/mTOR signaling, we next explored its functional target *in vitro*. Interestingly, ELISA indicated that LX2343 was a PI_3K inhibitor with an IC_{50} of 15.99±3.23 μmol/L (Figure 6C, 6D, Wortmannin as a positive control). Additionally, to test whether competition exists between LX2343 and ATP, we investigated the effects of ATP at different concentrations on the inhibitory activity of LX2343. The result demonstrated that the inhibition of LX2343 against PI_3K was virtually unaffected by ATP (Figure 6D). Thus, this result suggested that LX2343 is a non-ATP competitive inhibitor of PI_3K.

Considering that PI_3K regulates various processes in cell life, including cell growth, proliferation, differentiation, motility and survival and that most PI_3K inhibitors are used as anticancer drugs because of their cytotoxicity[45], we also detected the potential effect of LX2343 on cell viability, and the result

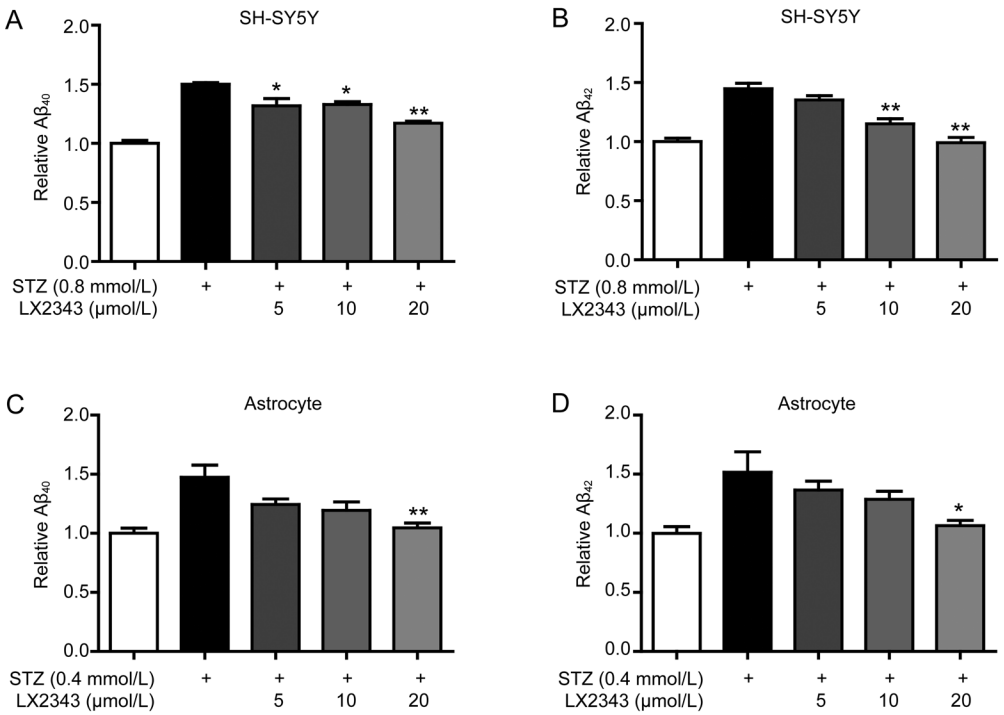

Figure 4. LX23434 promoted Aβ clearance. ELISA results indicated that LX2343 increased Aβ clearance in SH-SY5Y cells (A, B) and primary astrocytes (C, D) (one-way ANOVA, Dunnett's multiple comparison test. n=3. $^{*}P$<0.05, $^{**}P$<0.01 *vs* STZ). All data were obtained from three independent experiments and are presented as the mean±SEM.

indicated that LX2343 rendered few toxic effects on cells (Figure 6E).

In addition, given that many PI_3K inhibitors are being used as anticancer drugs and that some are autophagy stimulators that regulate the PI_3K/AKT/mTOR pathway, we also evaluated the extent of autophagy regulators on Aβ clearance based on PI3K-targeted anticancer drugs. In this assay, Idelalisib (CAL101), an anticancer drug that acts by inhibiting PI3K[46], was randomly selected for the study. Interestingly, the results demonstrated that the capability of LX2343 to promote autophagy was weaker compared to Idelalisib (Supplementary Figure S1A, S1B), but the ability of LX2343 to stimulate Aβ clearance was similar to the ability of Idelalisib (Supplementary Figure S1C–S1E). Here, we tentatively suggested that such the contrary efficiency of Idelalisib might be due to its cytotoxicity (Supplementary Figure S1F). Moreover, these results may also imply that not all PI_3K inhibitors that act as autophagy stimulators are suitable for AD treatment because of the complicated pivotal regulatory roles of PI3K in cell physiology.

Therefore, all of the results demonstrated that LX2343, as a PI_3K inhibitor, stimulated autophagy in its promotion of Aβ clearance.

LX2343 ameliorated learning and memory impairments in APP/PS1 transgenic mice

APP/PS1 mice express chimeric human Swedish mutant APP and a mutant human presenilin 1 protein and are widely used as an effective animal model for AD dementia[30]. Here, we evaluated the amelioration of memory impairment by LX2343 in this model using the MWM test.

As expected, the results revealed that in 8-d training trials, the path lengths and escape latencies used to find the platform for APP/PS1 transgenic mice were remarkably longer than those for non-transgenic mice, while 10 mg/kg LX2343 administration obviously antagonized the prolonged path lengths and escape latencies at d 7 and 8 (Figure 7A, 7B). In the probe trial assay, the LX2343-administered transgenic mice crossed over the hidden location of the platform more frequently compared with the vehicle-administered transgenic mice (Figure 7C, 7D). We carried out the animal experiments using two different doses of LX2343, 3 and 10 mg/kg. No improvement was detected in memory and learning in the 3 mg/kg treatment group (data not shown), which may indicate the dose-dependent effect of LX2343 *in vivo*.

Additionally, we also found that LX2343 treatment did not induce apparent changes in body weight, liver function or swimming speed of the tested mice (Supplementary Figure S2A–S2D).

LX2343 reduced senile plaque formation and Aβ levels in APP/PS1 transgenic mice

Given that senile plaque formation by aggregated Aβ is a main hallmark of AD and also one of the main criteria of the neuropathological-histological verification of AD[47], we next evaluated whether LX2343 reduced amyloid plaque formation

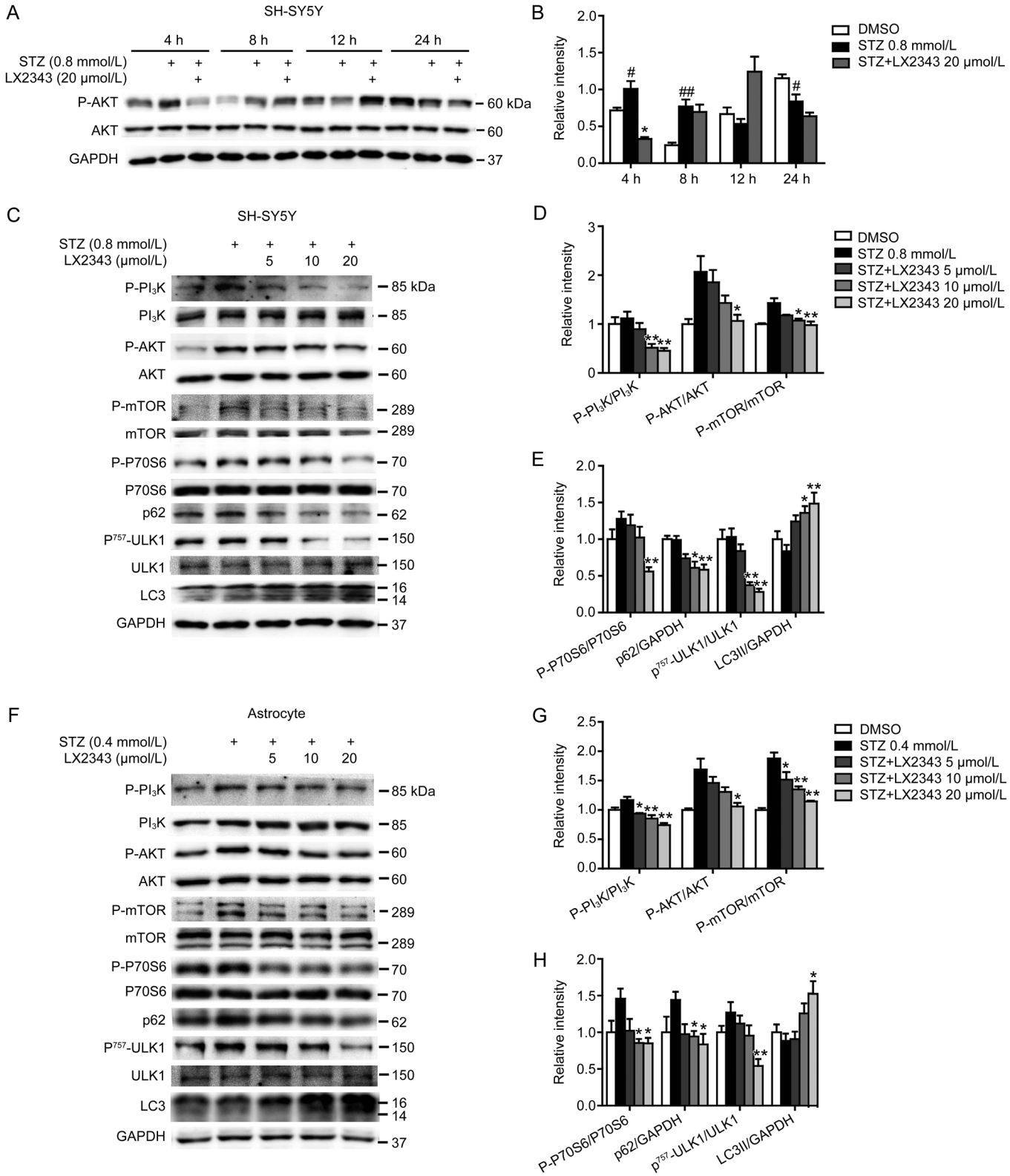

Figure 5. LX2343 inhibited PI_3K/AKT/mTOR signaling pathway. Western blotting and its quantification results indicated that a short duration of STZ stimulation led to increased phosphorylation of AKT in SH-SY5Y cell lysates (A, B) (*t* test. n=3. $^{*}P$<0.05 *vs* STZ. $^{\#}P$<0.05, $^{\#\#}P$<0.01 *vs* DMSO). Western blotting and its quantification results demonstrated that LX2343 reduced PI_3K, AKT, mTOR, P70S6, and ULK1 phosphorylation, decreased p62 protein levels, and promoted LC3 processing in SH-SY5Y cells (C–E) and in primary astrocytes (F–H) (one-way ANOVA, Dunnett's multiple comparison test. n=3. $^{*}P$<0.05, $^{**}P$<0.01 *vs* STZ). GAPDH was used as a loading control in the Western blot assays. All data were obtained from three independent experiments and are presented as the mean±SEM.

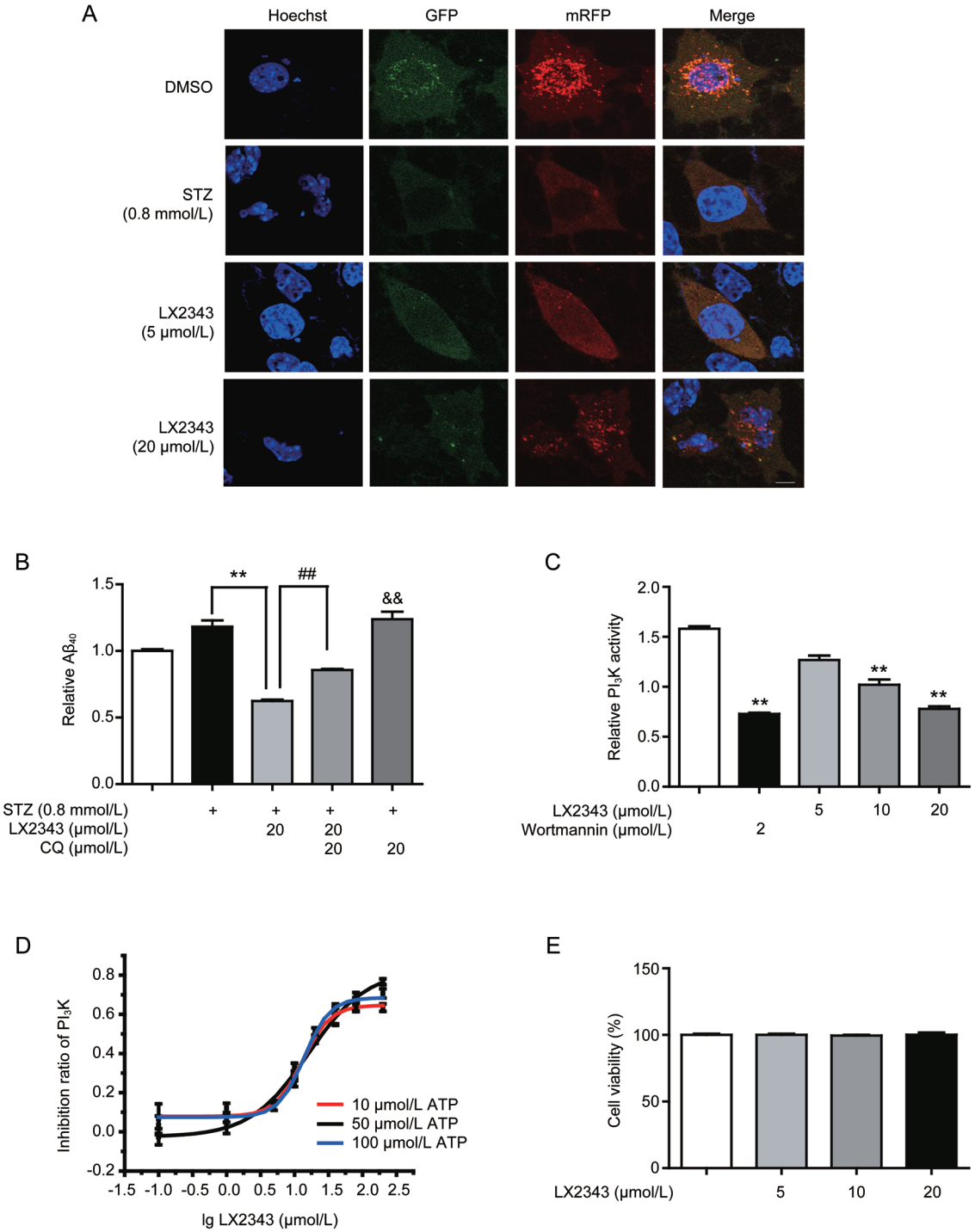

Figure 6. LX2343 as a PI_3K inhibitor stimulated autophagy in the promotion of Aβ clearance. CLSM images of SH-SY5Y cells transiently expressing mRFP-GFP-LC3 (A) (green and red puncta indicate GFP and mRFP, respectively. Scale bar: 5 μm, *n*=3). CQ-based ELISA result demonstrated that CQ enhanced Aβ levels and partially reversed LX2343-induced Aβ reduction in SH-SY5Y cells (B) (*t* test, $^{**}P$<0.01 *vs* STZ; $^{\#\#}P$<0.01 *vs* STZ combined with LX2343; $^{\&\&}P$<0.01 *vs* DMSO). LX2343 dose-dependently inhibited PI_3K activity *in vitro* (C) (wortmannin: PI_3K inhibitor. One-way ANOVA, Dunnett's multiple comparison test. *n*=3. $^{**}P$<0.01 *vs* DMSO; wortmannin, *t* test, *n*=3). LX2343 dose-dependently inhibited PI_3K in the presence of the indicated concentrations of ATP (D). In the presence of 10 μmol/L of ATP, the IC_{50} of LX2343 is 13.11±1.47 μmol/L, in the presence of 50 μmol/L ATP, the IC_{50} of LX2343 is 13.86±1.12 μmol/L, in the presence of 100 μmol/L ATP, the IC_{50} of LX2343 is 15.99±3.23 μmol/L. LX2343 concentration was expressed in log10 scale. MTT assay result demonstrated that LX2343 had no effects on cell viability in SH-SY5Y (E) (one-way ANOVA, Dunnett's multiple comparison test, *n*=3). GAPDH was used as loading control in Western blot assays. All data were obtained from three independent experiments and presented as mean±SEM.

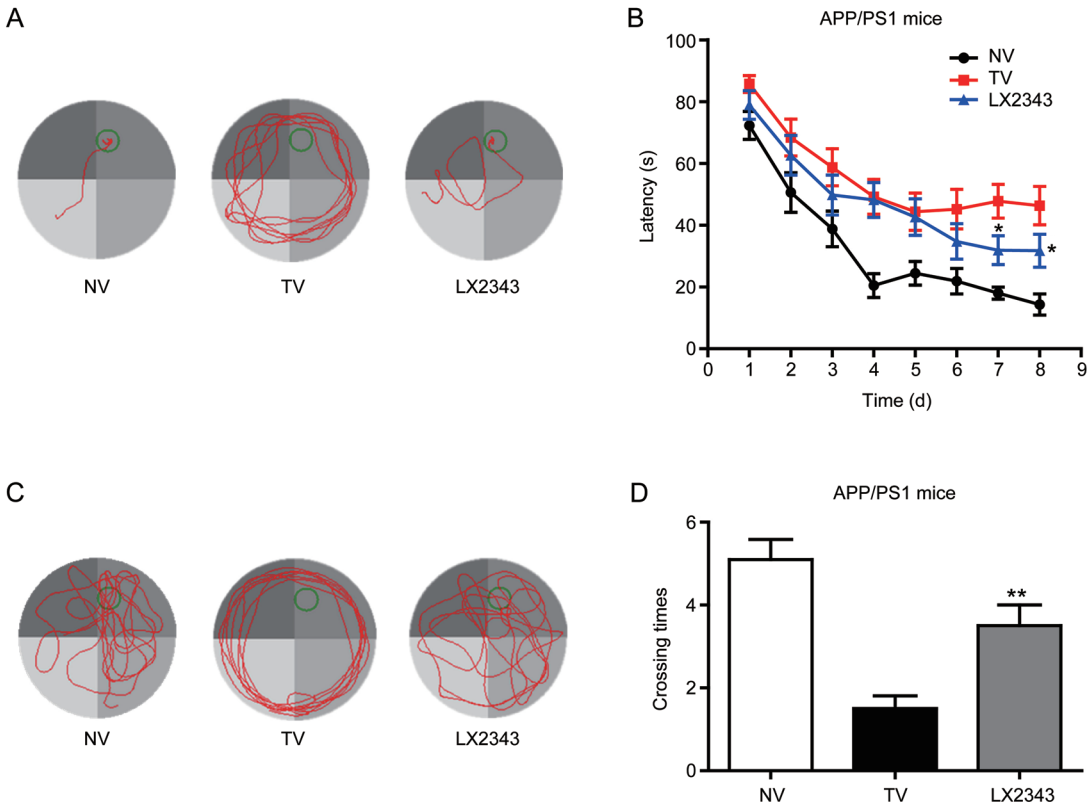

Figure 7. LX2343 effectively improved learning and memory impairments in APP/PS1 transgenic mice. Behavioral tests and quantitative analyses of the APP/PS1 transgenic mice. Representative tracing graphs showing the training trials (A). Escape latency during the platform trials in the MWM tests (B) (two-way ANOVA with repeated measures over time: treatment, $P<0.0001$; time, $P<0.0001$; treatment×time. $^{*}P<0.05$ *vs* TV. $n=10$). Representative tracing graphs of the probe trials (C). Times of the platform crossings in the probe trials (D) (*t* test, $^{**}P<0.01$ *vs* TV. $n=10$). NV: non-transgenic mice administered vehicle, TV: Transgenic mice administered vehicle LX2343: transgenic mice administered with 10 mg·kg^{-1}·d^{-1} of LX2343. Values are expressed as the mean±SEM.

in mice by performing thioflavine S staining assays, where senile plaque burdens were stained in green-fluorescence. The results demonstrated that the extent of amyloid plaques in the cerebral cortex or hippocampus of the APP/PS1 transgenic mice was more severe compared with that of non-transgenic mice, and LX2343 treatment efficiently reversed the effect (Figure 8A, 8B). Similarly, ELISA assays against $A\beta_{40/42}$ revealed higher levels of $A\beta_{40/42}$ in the cerebral cortex and hippocampus of transgenic mice compared with those of non-transgenic mice, while LX2343 administration suppressed Aβ levels (Figure 8C, 8D). Therefore, these results implied that LX2343 reduced senile plaque formation and Aβ levels in APP/PS1 transgenic mice.

LX2343 stimulated PI_3K/AKT/mTOR-mediated autophagy in APP/PS1 transgenic mice

Next, the promotion of LX2343 on Aβ clearance by activating PI_3K/AKT/mTOR-mediated autophagy was investigated in the cortex of APP/PS1 transgenic mice via Western blot analysis. The results indicated that the phosphorylation levels of PI_3K, AKT, mTOR, P70S6, and ULK1 and the protein level of p62 were higher, while the cleavage of LC3 was more restrained in transgenic mice compared to non-transgenic mice, indicating the suppression of autophagy[30]. LX2343 administration alleviated these effects, thus activating autophagy. These results demonstrated the efficacy of LX2343 in promoting PI_3K/AKT/mTOR-mediated autophagy in APP/PS1 transgenic mice (Figure 8E–8G).

LX2343 repressed JNK/APP^{Thr668}-mediated Aβ generation

Finally, we investigated the alleviation of LX2343 on Aβ production by inhibiting both JNK/APP^{Thr668} signaling and BACE1 enzymatic activity of APP/PS1 mice. Western blot results indicated that LX2343 administration decreased the phosphorylation levels of JNK and APP^{Thr668} and the levels of sAPPβ compared with vehicle-treated transgenic mice but had no effect on BACE1 protein levels (Figure 9A, 9B). In addition, the ELISA results also validated reductions in sAPPβ in the cerebral cortex and hippocampus of the transgenic mice treated with LX2343 (Figure 9C). However, we failed to identify BACE1 enzymatic inhibition compared with the vehicle-treated transgenic mice using a commercial kit (Materials and methods), which is likely due to the complicated tissue contents that might interrupt enzyme activity detection.

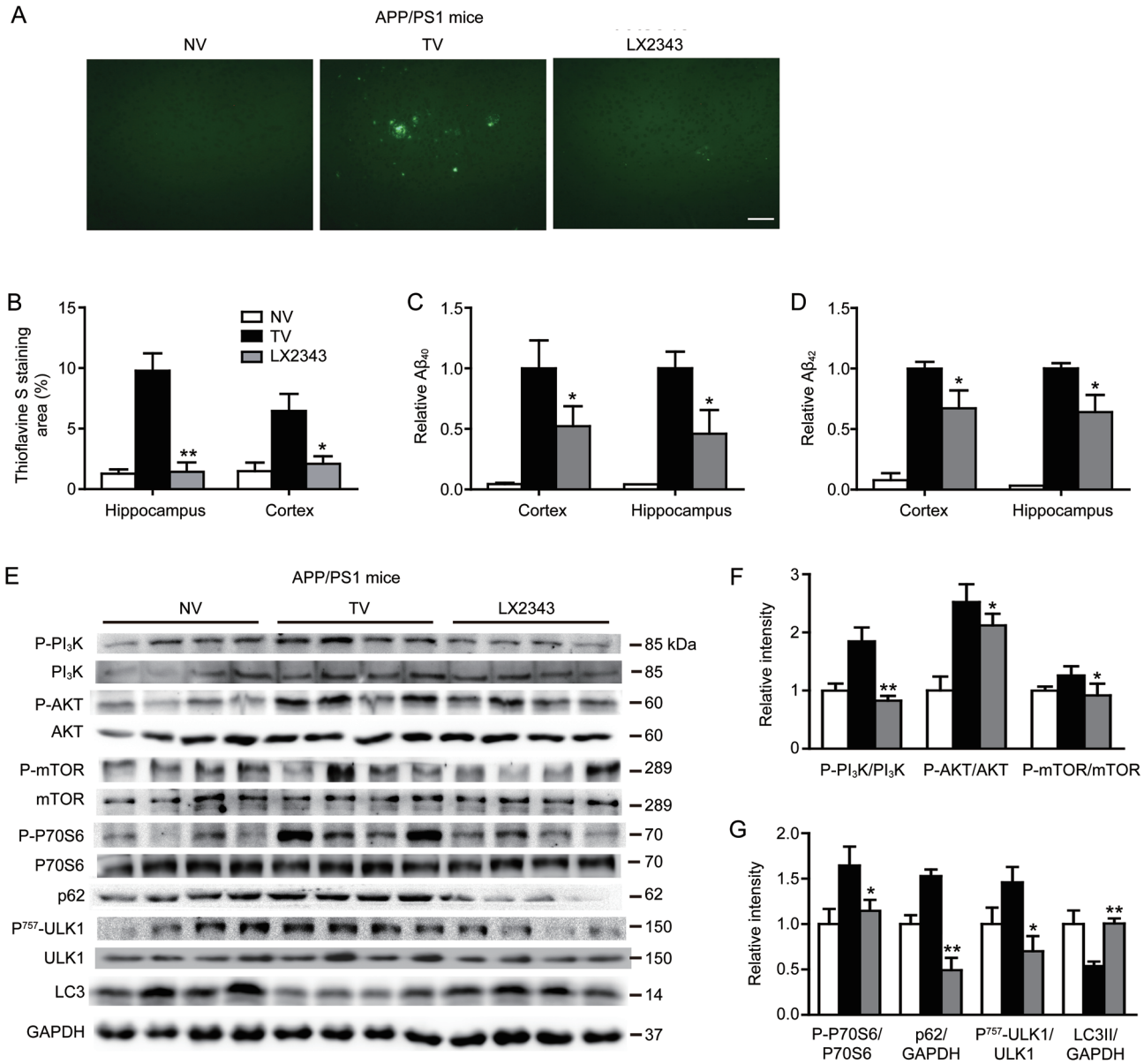

Figure 8. LX2343 reduced Aβ pathology by promoting PI_3K/AKT/mTOR-mediated autophagy in APP/PS1 transgenic mice. Representative micrographs of thioflavine S-stained amyloid plaques in the brains of APP/PS1 transgenic mice, scale bar: 100 μm (A). Statistical analysis of A (B) (*t* test. *n*=4. $^{*}P<0.05$, $^{**}P<0.01$ *vs* TV). ELISA results demonstrated that LX2343 decreased Aβ levels in the cortical and hippocampal homogenates of APP/PS1 transgenic mice (C, D) (*t* test. *n*=10. $^{*}P<0.05$ *vs* TV). Western blotting and its quantification results demonstrated that LX2343 reduced PI_3K, AKT, mTOR, P70S6, and ULK1 phosphorylation, decreased p62 protein levels, and promoted LC3 processing in the cortical homogenates of APP/PS1 transgenic mice (E–G) (*t* test. *n*=4. $^{*}P<0.05$, $^{**}P<0.01$ *vs* TV). GAPDH was used as a loading control in the Western blot assays. NV: non-transgenic mice administered vehicle, TV: transgenic mice administered vehicle; LX2343: transgenic mice administered with 10 $mg{\cdot}kg^{-1}{\cdot}d^{-1}$ of LX2343. Values are expressed as the mean±SEM.

LX2343 protected synaptic integrity

Given that Aβ accumulation may trigger aberrant network activity and synaptic depression accounting for cognitive decline in AD[48], we next examined the protein levels of PSD95, synaptophysin and VAMP2, which are three crucial proteins for neurotransmission and synaptic plasticity[49], to evaluate synaptic integrity and function in response to LX2343 administration. As expected, the results indicated that the administration of LX2343 efficiently reversed the suppression of the protein levels of PSD95, synaptophysin and VAMP2 in the cerebral cortex of transgenic mice compared with the vehicle-treated transgenic mice (Figure 9D, 9E), which thereby implied that LX2343 protected synaptic integrity and function.

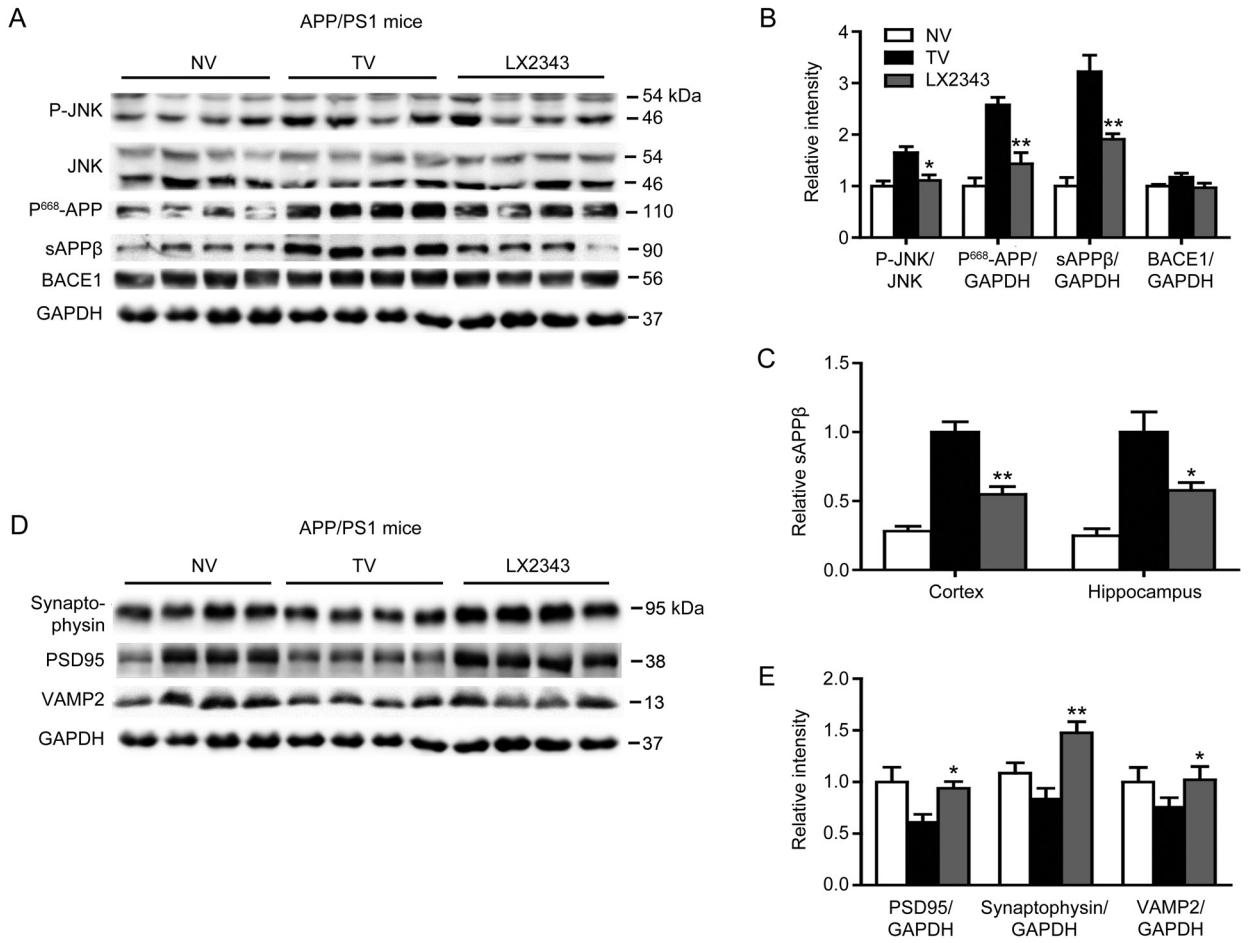

Figure 9. LX2343 repressed JNK/APP^{Thr668}-mediated Aβ generation and protected synaptic integrity in APP/PS1 transgenic mice. Western blotting and its quantification results demonstrated that LX2343 reduced the phosphorylation of JNK and APP^{Thr668}, decreased the protein level of sAPPβ, and had no effects on the protein level of BACE1 in cortical homogenates of APP/PS1 transgenic mice (A, B) (*t* test, *n*=4. $^{*}P$<0.05, $^{**}P$<0.01 *vs* TV). ELISA results demonstrated that LX2343 decreased the sAPPβ in cortex and hippocampus homogenates of APP/PS1 transgenic mice (C) (*t* test, *n*=10. $^{*}P$<0.05, $^{**}P$<0.01 *vs* TV). Western blotting and its quantification results demonstrated that LX2343 increased the protein levels of synaptophysin, PSD95 and VAMP2 in cortex homogenates of APP/PS1 transgenic mice (D, E) (*t* test, *n*=4. $^{*}P$<0.05, $^{**}P$<0.01 *vs* TV). GAPDH was used as loading control in Western blot assays. NV: nontransgenic mice administered with vehicle; TV: Transgenic mice administered with vehicle; LX2343: transgenic mice administered with 10 mg·kg^{-1}·d^{-1} LX2343. Values are mean±SEM.

LX2343 prolonged the lifespan of wild-type *Drosophila melanogaster*

According to previously published research, aging is a principal risk factor for the development and progression of AD, and delaying aging is an applicable strategy to decrease the rate of AD cases and to postpone AD progression[50]. Currently, several reports have published various proteins and signaling pathways involved in regulation of the aging process and longevity. For example, autophagy enhancement has been determined to prolong the lifespans of *Drosophila melanogaster*[51], and the mTOR inhibitor rapamycin extended the lifespans of mice[52]. Thus, given that LX2343 effectively enhanced autophagy, we examined the effect of LX2343 on the lifespans of wild-type *Drosophila melanogaster*. As expected, LX2343 administration potently prolonged the lifespans of *Drosophila melanogaster* (Figure 10A, 10B). This result thus showed that LX2343 also was able to prevent AD by delaying aging.

Discussion

In the current study, we determined that the small molecule LX2343 exhibited a high efficiency in alleviating Aβ levels and ameliorating memory deficits in APP/PS1 model mice. The results strongly highlighted the potential of LX2343 in the treatment of AD.

For many years, the amyloid cascade hypothesis has dominantly influenced the targets of drug discovery and has furthered drug development against AD[13]. However, the increasing number of recent failures of anti-amyloid agents in clinical trials have elicited a series of arguments against this hypothesis[13], and several researchers have postulated that the Aβ hypothesis may not be sufficient to recapitulate

A

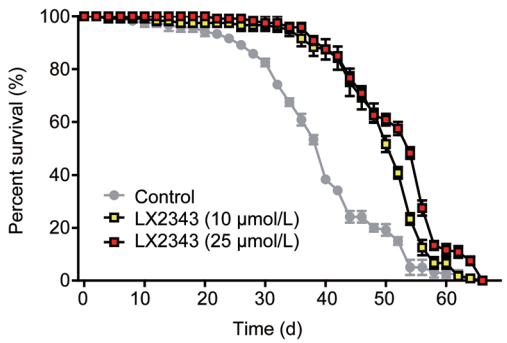

B

No	Dose	Mean lifespan (d)
Control (DMSO)	0.20%	42
LX2343	10 μmol/L	52
	25 μmol/L	54

Figure 10. LX2343 treatment extended the lifespan of wild-type *Drosophila melanogaster*. Survival of control and LX2343-treated wild-type *Drosophila melanogaster* (A). Statistical analysis of the mean lifespans in the groups treated or not treated with LX2343 (B).

AD pathogenesis[53–55]. In fact, most AD patients are sporadic, with only 1%–5% of cases that are due to familial AD, exhibiting genetic mutations in line with the initiator role of Aβ[56]. In addition, aging is also believed to be a potent risk factor for sporadic AD, which is characterized by a distinct etiology from familial AD[57]. It is thus suggested that Aβ accumulation is an adaptive response to chronic brain stress, and prolonged stress stimulation might be highly involved in the pathogenic events of sporadic AD[58, 59]. Therefore, a potential Aβ modulator should be evaluated based on a full spectrum of the pathologies of AD[55] rather than using a simple model in healthy primary or immortal cells because this model is not sufficient to reflect the actual intricate pathological situations *in vivo*. Therefore, here, we constructed a compound-screening platform using STZ to induce pathological events of AD that included oxidative stress and Aβ/tau pathology. We discovered that LX2343 exhibited high activity in Aβ inhibition and cognitive improvement in APP/PS1 transgenic mice. The results revealed the efficiency of the current strategy in the search for anti-amyloid agents.

In the current study, we employed three types of immortal cells, CHO-APP, HEK293-APP_{sw} and SH-SY5Y cells. Although these cells are tumor-derived and may not completely recapitulate the properties of endogenous cells[60], their respective advantages may help complement each other in the assays. We did not use primary neurons because of their relatively low expression levels of Aβ and the restrictions in cell number[61, 62]. In the current study, spontaneous over-expression of Aβ was needed to evaluate the Aβ inhibition activity of the compound, while the high Aβ expression of CHO-APP and HEK293-APP_{sw} cells may facilitate the assays. Additionally, in Aβ clearance assays, SH-SY5Y cells, a neuroblastoma cell line that closely resembles primary neurons, was used instead of primary neurons[62]. Because primary astrocytes play an important role in autophagy-mediated Aβ clearance *in vivo* and are considered more suitable for the related assay[63], primary astrocytes were thus applied to further confirm the results obtained in the SH-SY5Y cells.

APP is a trans-membrane protein synthesized in the endoplasmic reticulum and transported through the Golgi network via secretory pathways[64]. The subcellular localization of APP is regulated by its phosphorylation at a number of sites, including Tyr-653, Thr-654, Ser-655, Ser-675, Thr-668, Tyr-682, Thr-686, and Tyr-687[65], while phosphorylation of APP^{Thr668} results in a significant conformational change and internalization into endosomal compartments, wherein it undergoes amyloidogenic processing[33]. Recently, it was demonstrated that APP^{Thr668} phosphorylation can be mediated by JNK, a kinase with multiple functions in apoptosis and inflammation[66], leading to a promotion of Aβ production, which further stimulates JNK activity[33]. Here, we found that LX2343 reduced amyloidogenic cleavage by inhibiting JNK, which supports the potential of JNK inhibitors in the treatment of AD[7].

BACE1, as a rate-limiting enzyme for Aβ production[67], is a traditional target for anti-amyloid drug discovery. In the present study, we demonstrated that LX2343 is also a BACE1 enzyme inhibitor. Although the efficiency of LX2343 in BACE1 inhibition was less potent than that of the positive compound TDC[28] (Figure 2G), the dual effects of LX2343 on both the JNK/APP pathway and on BACE1 inhibition synergistically contributed to its high capability in restraining Aβ production.

Defective autophagy is linked to several age-dependent neurodegenerative diseases[68], including AD[69], and autophagy enhancement may prolong the lifespans of *Drosophila melanogaster*[51] and extend the lifespans of mice[52], and the agents able to activate autophagy have been identified to delay AD pathological processes and to rescue memory impairment in AD model mice[70]. Our result that LX2343 as an effective autophagy activator potently prolonged the lifespan of *Drosophila melanogaster* thus strongly supported its potential capability in the prevention of AD by delaying aging.

In summary, we reported that LX2343 effectively ameliorated cognitive dysfunction in APP/PS1 transgenic mice, and the underlying mechanisms were intensively investigated. As summarized in the proposed schematic diagram, LX2343 reduced Aβ production by both inhibiting APP cleavage through the inhibition of JNK-mediated APP^{Thr668} phosphorylation and by suppressing BACE1 activity while also increasing Aβ clearance by functioning as a PI_3K inhibitor to negatively regulate PI_3K/AKT/mTOR signaling in the promotion of autophagy (Figure 11). All of the results thereby demonstrate the potential of LX2343 in the treatment of AD.

Acknowledgements

We thank Prof Hai-yun SONG (Institute for Nutritional Sciences, Chinese Academy of Sciences, Shanghai, China) for help

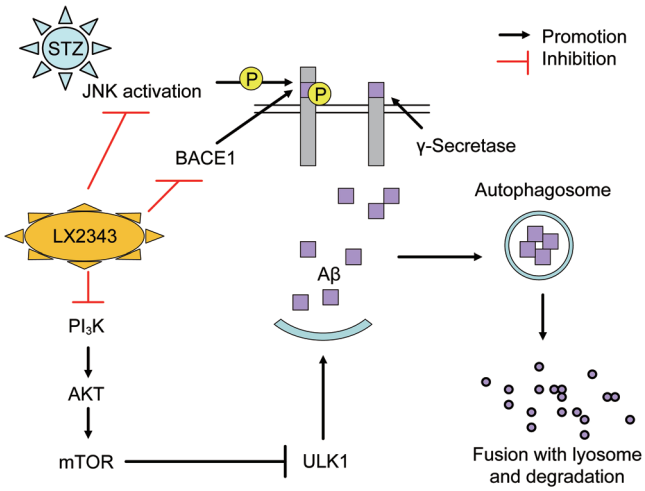

Figure 11. A proposed model illustrating the mechanism underlying LX2343-mediated Aβ production inhibition and Aβ clearance promotion. Aβ is produced from the sequential cleavage of APP by BACE1 and γ-secretase. It can be degraded using autophagy. LX2343 synergistically restrains Aβ production by both inhibiting APP cleavage through the inhibition of JNK-mediated APP^{Thr668} phosphorylation and by suppressing BACE1 activity. In addition, LX2343, as a PI_3K inhibitor, enhances Aβ clearance by stimulating autophagy through PI_3K/AKT/mTOR pathway inhibition.

with the lifespan experiments in *Drosophila melanogaster*. This work was supported by the National Natural Science Foundation of China (81220108025, 81473141, and 81273556), NSFC-TRF collaboration projects (81561148011 and DBG5980001) and the Drug Innovation Project of SIMM (CASIMM0120154035).

Author contribution

Xu SHEN, Zhi-yuan ZHU, and Xiao-dan GUO designed the experiment; Xiao-dan GUO carried out the experiments and analyzed the data; Guang-long SUN and Li-hong HU synthesized the compound; Ting-ting ZHOU and Xin XU participated in animal sacrificing; Xu SHEN and Xiao-dan GUO wrote the manuscript; all authors, including Vatcharin RUKACHAISIRIKUL, discussed the results and contributed to the revision of the final manuscript.

Supplementary information

Supplementary Figures are available on the website of Acta Pharmacologica Sinica.

References

1 Hardy J. A hundred years of Alzheimer's disease research. Neuron 2006; 52: 3–13.
2 Thies W, Bleiler L, Alzheimer's A. 2013 Alzheimer's disease facts and figures. Alzheimers Dement 2013; 9: 208–45.
3 Musiek ES, Holtzman DM. Three dimensions of the amyloid hypothesis: time, space and 'wingmen'. Nat Neurosci 2015; 18: 800–6.
4 Hardy J, Allsop D. Amyloid deposition as the central event in the aetiology of Alzheimer's disease. Trends Pharmacol Sci 1991; 12: 383–8.
5 Huang Y, Mucke L. Alzheimer mechanisms and therapeutic strategies. Cell 2012; 148: 1204–22.
6 Bero AW, Yan P, Roh JH, Cirrito JR, Stewart FR, Raichle ME, *et al.* Neuronal activity regulates the regional vulnerability to amyloid-beta deposition. Nat Neurosci 2011; 14: 750–6.
7 Guo X, Jiang W, Li C, Zhu Z, Shen X. Abeta regulation-based multitarget strategy for drug discovery against Alzheimer's disease. Rev Neurosci 2015; 26: 13–30.
8 Vincent B, Govitrapong P. Activation of the alpha-secretase processing of AbetaPP as a therapeutic approach in Alzheimer's disease. J Alzheimers Dis 2011; 24: 75–94.
9 Pettersson M, Stepan AF, Kauffman GW, Johnson DS. Novel gamma-secretase modulators for the treatment of Alzheimer's disease: a review focusing on patents from 2010 to 2012. Expert Opin Ther Pat 2013; 23: 1349–66.
10 Nie Q, Du XG, Geng MY. Small molecule inhibitors of amyloid beta peptide aggregation as a potential therapeutic strategy for Alzheimer's disease. Acta Pharmacol Sin 2011; 32: 545–51.
11 Lichtenthaler SF. alpha-secretase in Alzheimer's disease: molecular identity, regulation and therapeutic potential. J Neurochem 2011; 116: 10–21.
12 Forman M, Tseng J, Palcza J, Leempoels J, Ramael S, Krishna G, *et al.* The novel BACE inhibitor MK-8931 dramatically lowers CSF A beta peptides in healthy subjects: results from a rising single dose study. Neurology 2012; 78.
13 Schneider LS, Mangialasche F, Andreasen N, Feldman H, Giacobini E, Jones R, *et al.* Clinical trials and late-stage drug development for Alzheimer's disease: an appraisal from 1984 to 2014. J Intern Med 2014; 275: 251–83.
14 Hardy J, Bogdanovic N, Winblad B, Portelius E, Andreasen N, Cedazo-Minguez A, *et al.* Pathways to Alzheimer's disease. J Intern Med 2014; 275: 296–303.
15 Schellenberg GD, Montine TJ. The genetics and neuropathology of Alzheimer's disease. Acta Neuropathol 2012; 124: 305–23.
16 Buccafusco JJ, Terry AV Jr. Multiple central nervous system targets for eliciting beneficial effects on memory and cognition. J Pharmacol Exp Ther 2000; 295: 438–46.
17 Clark TA, Lee HP, Rolston RK, Zhu X, Marlatt MW, Castellani RJ, *et al.* Oxidative stress and its implications for future treatments and management of Alzheimer disease. Int J Biomed Sci 2010; 6: 225–7.
18 Kim GH, Kim JE, Rhie SJ, Yoon S. The role of oxidative stress in neurodegenerative diseases. Exp Neurobiol 2015; 24: 325–40.
19 Guan ZZ. Cross-talk between oxidative stress and modifications of cholinergic and glutaminergic receptors in the pathogenesis of Alzheimer's disease. Acta Pharmacol Sin 2008; 29: 773–80.
20 Tiraboschi P, Hansen LA, Thal LJ, Corey-Bloom J. The importance of neuritic plaques and tangles to the development and evolution of AD. Neurology 2004; 62: 1984–9.
21 Salkovic-Petrisic M, Knezovic A, Hoyer S, Riederer P. What have we learned from the streptozotocin-induced animal model of sporadic Alzheimer's disease, about the therapeutic strategies in Alzheimer's research. J Neural Transm (Vienna) 2013; 120: 233–52.
22 Biswas J, Goswami P, Gupta S, Joshi N, Nath C, Singh S. Streptozotocin induced neurotoxicity involves Alzheimer's related pathological markers: a study on N2A cells. Mol Neurobiol 2016; 53: 2794–806.
23 Yang S, Xia C, Li S, Du L, Zhang L, Hu Y. Mitochondrial dysfunction driven by the LRRK2-mediated pathway is associated with loss of Purkinje cells and motor coordination deficits in diabetic rat model. Cell Death Dis 2014; 5: e1217.
24 Zhu Z, Yan J, Jiang W, Yao XG, Chen J, Chen L, *et al.* Arctigenin effectively ameliorates memory impairment in Alzheimer's disease

model mice targeting both beta-amyloid production and clearance. J Neurosci 2013; 33: 13138–49.
25 Deeds MC, Anderson JM, Armstrong AS, Gastineau DA, Hiddinga HJ, Jahangir A, *et al.* Single dose streptozotocin-induced diabetes: considerations for study design in islet transplantation models. Lab Anim 2011; 45: 131–40.
26 Jiang Q, Lee CY, Mandrekar S, Wilkinson B, Cramer P, Zelcer N, *et al.* ApoE promotes the proteolytic degradation of Abeta. Neuron 2008; 58: 681–93.
27 Cramer PE, Cirrito JR, Wesson DW, Lee CY, Karlo JC, Zinn AE, *et al.* ApoE-directed therapeutics rapidly clear beta-amyloid and reverse deficits in AD mouse models. Science 2012; 335: 1503–6.
28 Zhu Z, Li C, Wang X, Yang Z, Chen J, Hu L, *et al.* 2,2′,4′-trihydroxychalcone from *Glycyrrhiza glabra* as a new specific BACE1 inhibitor efficiently ameliorates memory impairment in mice. J Neurochem 2010; 114: 374–85.
29 Malumbres M, Mangues R, Ferrer N, Lu S, Pellicer A. Isolation of high molecular weight DNA for reliable genotyping of transgenic mice. Biotechniques 1997; 22: 1114–9.
30 Reiserer RS, Harrison FE, Syverud DC, McDonald MP. Impaired spatial learning in the APP_{Swe}+PSEN1DeltaE9 bigenic mouse model of Alzheimer's disease. Genes Brain Behav 2007; 6: 54–65.
31 Colombo A, Bastone A, Ploia C, Sclip A, Salmona M, Forloni G*, et al.* JNK regulates APP cleavage and degradation in a model of Alzheimer's disease. Neurobiol Dis 2009; 33: 518–25.
32 Yoon SO, Park DJ, Ryu JC, Ozer HG, Tep C, Shin YJ*, et al.* JNK3 perpetuates metabolic stress induced by Abeta peptides. Neuron 2012; 75: 824–37.
33 Mazzitelli S, Xu P, Ferrer I, Davis RJ, Tournier C. The loss of c-Jun N-terminal protein kinase activity prevents the amyloidogenic cleavage of amyloid precursor protein and the formation of amyloid plaques *in vivo*. J Neurosci 2011; 31: 16969–76.
34 Klionsky DJ, Emr SD. Autophagy as a regulated pathway of cellular degradation. Science 2000; 290: 1717–21.
35 Chan EY, Kir S, Tooze SA. siRNA screening of the kinome identifies ULK1 as a multidomain modulator of autophagy. J Biol Chem 2007; 282: 25464–74.
36 Nave BT, Ouwens M, Withers DJ, Alessi DR, Shepherd PR. Mammalian target of rapamycin is a direct target for protein kinase B: identification of a convergence point for opposing effects of insulin and amino-acid deficiency on protein translation. Biochem J 1999; 344: 427–31.
37 Memmott RM, Dennis PA. Akt-dependent and -independent mechanisms of mTOR regulation in cancer. Cell Signal 2009; 21: 656–64.
38 Franke TF, Kaplan DR, Cantley LC, Toker A. Direct regulation of the Akt proto-oncogene product by phosphatidylinositol-3,4-bisphosphate. Science 1997; 275: 665–8.
39 Xiao T, Guan X, Nie L, Wang S, Sun L, He T*, et al.* Rapamycin promotes podocyte autophagy and ameliorates renal injury in diabetic mice. Mol Cell Biochem 2014; 394: 145–54.
40 Zhao Y, Zhang L, Qiao Y, Zhou X, Wu G, Wang L, *et al.* Heme oxygenase-1 prevents cardiac dysfunction in streptozotocin-diabetic mice by reducing inflammation, oxidative stress, apoptosis and enhancing autophagy. PLoS One 2013; 8: e75927.
41 Matthews JA, Belof JL, Acevedo-Duncan M, Potter RL. Glucosamine-induced increase in Akt phosphorylation corresponds to increased endoplasmic reticulum stress in astroglial cells. Mol Cell Biochem 2007; 298: 109–23.
42 Bjorkoy G, Lamark T, Brech A, Outzen H, Perander M, Overvatn A*, et al.* p62/SQSTM1 forms protein aggregates degraded by autophagy and has a protective effect on huntingtin-induced cell death. J Cell Biol 2005; 171: 603–14.
43 Kimura S, Noda T, Yoshimori T. Dissection of the autophagosome maturation process by a novel reporter protein, tandem fluorescent-tagged LC3. Autophagy 2007; 3: 452–60.
44 Kimura T, Takabatake Y, Takahashi A, Isaka Y. Chloroquine in cancer therapy: a double-edged sword of autophagy. Cancer Res 2013; 73: 3–7.
45 Lee JJ, Loh K, Yap YS. PI3K/Akt/mTOR inhibitors in breast cancer. Cancer Biol Med 2015; 12: 342–54.
46 Ikeda H, Hideshima T, Fulciniti M, Perrone G, Miura N, Yasui H, *et al.* PI3K/p110{delta} is a novel therapeutic target in multiple myeloma. Blood 2010; 116: 1460–8.
47 Araujo DM, Cotman CW. Beta-amyloid stimulates glial cells *in vitro* to produce growth factors that accumulate in senile plaques in Alzheimer's disease. Brain Res 1992; 569: 141–5.
48 Rai S, Kamat PK, Nath C, Shukla R. Glial activation and post-synaptic neurotoxicity: the key events in Streptozotocin (ICV) induced memory impairment in rats. Pharmacol Biochem Behav 2014; 117: 104–17.
49 Valtorta F, Pennuto M, Bonanomi D, Benfenati F. Synaptophysin: leading actor or walk-on role in synaptic vesicle exocytosis? Bioessays 2004; 26: 445–53.
50 Jirillo E, Candore G, Magrone T, Caruso C. A scientific approach to anti-ageing therapies: state of the art. Curr Pharm Des 2008; 14: 2637–42.
51 Simonsen A, Cumming RC, Brech A, Isakson P, Schubert DR, Finley KD. Promoting basal levels of autophagy in the nervous system enhances longevity and oxidant resistance in adult *Drosophila*. Autophagy 2008; 4: 176–84.
52 Harrison DE, Strong R, Sharp ZD, Nelson JF, Astle CM, Flurkey K, *et al.* Rapamycin fed late in life extends lifespan in genetically heterogeneous mice. Nature 2009; 460: 392–5.
53 Castello MA, Jeppson JD, Soriano S. Moving beyond anti-amyloid therapy for the prevention and treatment of Alzheimer's disease. BMC Neurol 2014; 14: 169.
54 Puzzo D, Gulisano W, Arancio O, Palmeri A. The keystone of Alzheimer pathogenesis might be sought in Abeta physiology. Neuroscience 2015; 307: 26–36.
55 Herrup K. The case for rejecting the amyloid cascade hypothesis. Nat Neurosci 2015; 18: 794–9.
56 Daviglus ML, Bell CC, Berrettini W, Bowen PE, Connolly ES Jr, Cox NJ, *et al.* National institutes of health state-of-the-science conference statement: preventing alzheimer disease and cognitive decline. Ann Intern Med 2010; 153: 176–81.
57 Herrup K. Reimagining Alzheimer's disease — an age-based hypothesis. J Neurosci 2010; 30: 16755–62.
58 Castello MA, Soriano S. On the origin of Alzheimer's disease. Trials and tribulations of the amyloid hypothesis. Ageing Res Rev 2014; 13: 10–2.
59 Stranahan AM, Mattson MP. Recruiting adaptive cellular stress responses for successful brain ageing. Nat Rev Neurosci 2012; 13: 209–16.
60 Gordon J, Amini S, White MK. General overview of neuronal cell culture. Methods Mol Biol 2013; 1078: 1–8.
61 Groemer TW, Thiel CS, Holt M, Riedel D, Hua Y, Huve J, *et al.* Amyloid precursor protein is trafficked and secreted via synaptic vesicles. PLoS One 2011; 6: e18754.
62 Kovalevich J, Langford D. Considerations for the use of SH-SY5Y neuroblastoma cells in neurobiology. Methods Mol Biol 2013; 1078: 9–21.
63 Bhat R, Crowe EP, Bitto A, Moh M, Katsetos CD, Garcia FU*, et al.* Astrocyte senescence as a component of Alzheimer's disease. PLoS

One 2012; 7: e45069.

64 Acevedo KM, Opazo CM, Norrish D, Challis LM, Li QX, White AR, *et al*. Phosphorylation of amyloid precursor protein at threonine 668 is essential for its copper-responsive trafficking in SH-SY5Y neuroblastoma cells. J Biol Chem 2014; 289: 11007–19.

65 Suzuki T, Nakaya T. Regulation of amyloid beta-protein precursor by phosphorylation and protein interactions. J Biol Chem 2008; 283: 29633–7.

66 Mehan S, Meena H, Sharma D, Sankhla R. JNK: a stress-activated protein kinase therapeutic strategies and involvement in Alzheimer's and various neurodegenerative abnormalities. J Mol Neurosci 2011; 43: 376–90.

67 Cai H, Wang Y, McCarthy D, Wen H, Borchelt DR, Price DL, *et al*. BACE1 is the major beta-secretase for generation of Abeta peptides by neurons. Nat Neurosci 2001; 4: 233–4.

68 He LQ, Lu JH, Yue ZY. Autophagy in ageing and ageing-associated diseases. Acta Pharmacol Sin 2013; 34: 605–11.

69 Nixon RA, Yang DS. Autophagy failure in Alzheimer's disease — locating the primary defect. Neurobiol Dis 2011; 43: 38–45.

70 Hochfeld WE, Lee S, Rubinsztein DC. Therapeutic induction of autophagy to modulate neurodegenerative disease progression. Acta Pharmacol Sin 2013; 34: 600–4.